reports about brain atrophy, but we must be cautious with the possibility that the registration errors may have an undefined contribution to the result of the comparison between the groups.

5 Conclusion

To the best of our knowledge, this is the first study to show that sensitivity for regional gray-matter volume change in the DMN is improved by the use of standardized analysis with global gray-matter volume, and to report longitudinal change for gray-matter volumes of the subdivided DMN (posterior cingulate, precuneus, LTC, MPFC, and IPL) in normal and converted (from MCI to AD) groups. The results are useful for improving our understanding of the features of regional gray-matter volume indication methods and for improving our understanding of DMN volume changes in the converted (from MCI to AD) phase.

Acknowledgments This study was supported by a Grant-in-Aid for Scientific Research on Innovative Areas (Comprehensive Brain Science Network) from the Ministry of Education, Science, Sports and Culture of Japan.

Conflict of interest We declare that we have no conflicts of interest.

References

1. Biswal BB, Van Kylen J, Hyde JS. Simultaneous assessment of flow and bold signals in resting-state functional connectivity maps. NMR Biomed. 1997;10:165–70.
2. Greicius MD, Krasnow B, Reiss AL, Menon V. Functional connectivity in the resting brain: a network analysis of the default mode hypothesis. Proc Natl Acad Sci USA. 2003;100:253–8.
3. Fox MD, Corbetta M, Snyder AZ, Vincent JL, Raichle ME. Spontaneous neuronal activity distinguishes human dorsal and ventral attention systems. Proc Natl Acad Sci USA. 2006; 103:10046–51.
4. Golland Y, Bentin S, Gelbard H, Benjamini Y, Heller R, Nir Y, et al. Extrinsic and intrinsic systems in the posterior cortex of the human brain revealed during natural sensory stimulation. Cereb Cortex. 2007;17:766–77.
5. Seeley WW, Menon V, Schatzberg AF, Keller J, Glover GH, Kenna H, et al. Dissociable intrinsic connectivity networks for salience processing and executive control. J Neurosci. 2007;27:2349–56.
6. Gusnard DA, Raichle ME. Searching for a baseline: functional imaging and the resting human brain. Nat Rev Neurosci. 2001;2:685–94.
7. Raichle ME, MacLeod AM, Snyder AZ, Powers WJ, Gusnard DA, Shulman GL. A default mode of brain function. Proc Natl Acad Sci USA. 2001;98:676–82.
8. Binder JR, Frost JA, Hammeke TA, Bellgowan PS, Rao SM, Cox RW. Conceptual processing during the conscious resting state. A functional MRI study. J Cogn Neurosci. 1999;11:80–95.
9. Shulman GL, Corbetta M, Buckner RL, Raichle ME, Fiez JA, Miezin FM, et al. Top-down modulation of early sensory cortex. Cereb Cortex. 1997;7:193–206.
10. Polli FE, Barton JJ, Cain MS, Thakkar KN, Rauch SL, Manoach DS. Rostral and dorsal anterior cingulate cortex make dissociable contributions during antisaccade error commission. Proc Natl Acad Sci USA. 2005;102:15700–5.
11. Fransson P. Spontaneous low-frequency bold signal fluctuations: an fMRI investigation of the resting-state default mode of brain function hypothesis. Hum Brain Mapp. 2005;26:15–29.
12. Greicius MD, Srivastava G, Reiss AL, Menon V. Default-mode network activity distinguishes alzheimer's disease from healthy aging: evidence from functional MRI. Proc Natl Acad Sci USA. 2004;101:4637–42.
13. Mosconi L. Brain glucose metabolism in the early and specific diagnosis of Alzheimer's disease. FDG-pet studies in mci and ad. Eur J Nucl Med Mol Imaging. 2005;32:486–510.
14. Buckner RL, Andrews-Hanna JR, Schacter DL. The brain's default network: anatomy, function, and relevance to disease. Ann N Y Acad Sci. 2008;1124:1–38.
15. Rombouts SA, Damoiseaux JS, Goekoop R, Barkhof F, Scheltens P, Smith SM, et al. Model-free group analysis shows altered bold fMRI networks in dementia. Hum Brain Mapp. 2009;30:256–66.
16. Wermke M, Sorg C, Wohlschlager AM, Drzezga A. A new integrative model of cerebral activation, deactivation and default mode function in Alzheimer's disease. Eur J Nucl Med Mol Imaging. 2008;35(Suppl 1):S12–24.
17. Fleisher AS, Sherzai A, Taylor C, Langbaum JB, Chen K, Buxton RB. Resting-state bold networks versus task-associated functional MRI for distinguishing Alzheimer's disease risk groups. Neuroimage. 2009;47:1678–90.
18. McCaffrey P, Fagan T, Landhuis E. Alzheimer research series on the default network. J Alzheimers Dis. 2010;19:747–58.
19. Zhang D, Raichle ME. Disease and the brain's dark energy. Nat Rev Neurol. 2010;6:15–28.
20. Shin J, Kepe V, Small GW, Phelps ME, Barrio JR. Multimodal imaging of Alzheimer pathophysiology in the brain's default mode network. Int: J Alzheimers Dis; 2011. p. 687945.
21. Maldjian JA, Laurienti PJ, Kraft RA, Burdette JH. An automated method for neuroanatomic and cytoarchitectonic atlas-based interrogation of fMRI data sets. Neuroimage. 2003;19:1233–9.
22. Ashburner J, Friston KJ. Unified segmentation. Neuroimage. 2005;26:839–51.
23. Tzourio-Mazoyer N, Landeau B, Papathanassiou D, Crivello F, Etard O, Delcroix N, et al. Automated anatomical labeling of activations in SPM using a macroscopic anatomical parcellation of the MNI MRI single-subject brain. Neuroimage. 2002; 15:273–89.
24. Petersen RC, Stevens JC, Ganguli M, Tangalos EG, Cummings JL, DeKosky ST. Practice parameter: early detection of dementia: mild cognitive impairment (an evidence-based review). Report of the Quality Standards Subcommittee of the American Academy of Neurology. Neurology. 2001;56:1133–42.
25. Goto M, Abe O, Aoki S, Takao H, Hayashi N, Miyati T, et al. Database of normal Japanese gray matter volumes in the default mode network. J Magn Reson Imaging. 2014;39:132–42.
26. Baron JC, Chetelat G, Desgranges B, Perchey G, Landeau B, de la Sayette V, et al. In vivo mapping of gray-matter loss with voxel-based morphometry in mild Alzheimer's disease. Neuroimage. 2001;14:298–309.
27. Matsuda H, Kitayama N, Ohnishi T, Asada T, Nakano S, Sakamoto S, et al. Longitudinal evaluation of both morphologic and functional changes in the same individuals with Alzheimer's disease. J Nucl Med. 2002;43:304–11.
28. Busatto GF, Garrido GE, Almeida OP, Castro CC, Camargo CH, Cid CG, et al. A voxel-based morphometry study of temporal lobe gray-matter reductions in Alzheimer's disease. Neurobiol Aging. 2003;24:221–31.

29. Chetelat G, Desgranges B, De La Sayette V, Viader F, Eustache F, Baron JC. Mapping gray-matter loss with voxel-based morphometry in mild cognitive impairment. NeuroReport. 2002;13:1939–43.
30. Frisoni GB, Testa C, Zorzan A, Sabattoli F, Beltramello A, Soininen H, et al. Detection of grey matter loss in mild Alzheimer's disease with voxel based morphometry. J Neurol Neurosurg Psychiatry. 2002;73:657–64.
31. Fortea J, Sala-Llonch R, Bartres-Faz D, Bosch B, Llado A, Bargallo N, et al. Increased cortical thickness and caudate volume precede atrophy in psen1 mutation carriers. J Alzheimers Dis. 2010;22:909–22.
32. Fortea J, Sala-Llonch R, Bartres-Faz D, Llado A, Sole-Padulles C, Bosch B, et al. Cognitively preserved subjects with transitional cerebrospinal fluid SS-amyloid 1–42 values have thicker cortex in Alzheimer's disease vulnerable areas. Biol Psychiatry. 2011;70: 183–90.
33. Hyman BT, Gomez-Isla T. Alzheimer's disease is a laminar, regional, and neural system specific disease, not a global brain disease. Neurobiol Aging. 1994;15:353–4.
34. De Lacoste MC, White CL 3rd. The role of cortical connectivity in Alzheimer's disease pathogenesis: a review and model system. Neurobiol Aging. 1993;14:1–16.
35. Berg L, McKeel DW Jr, Miller JP, Storandt M, Rubin EH, Morris JC, et al. Clinicopathologic studies in cognitively healthy aging and Alzheimer's disease: relation of histologic markers to dementia severity, age, sex, and apolipoprotein e genotype. Arch Neurol. 1998;55:326–35.
36. Hedden T, Van Dijk KR, Becker JA, Mehta A, Sperling RA, Johnson KA, et al. Disruption of functional connectivity in clinically normal older adults harboring amyloid burden. J Neurosci. 2009;29:12686–94.
37. Sheline YI, Raichle ME, Snyder AZ, Morris JC, Head D, Wang S, et al. Amyloid plaques disrupt resting state default mode network connectivity in cognitively normal elderly. Biol Psychiatry. 2010;67:584–7.
38. Petrella JR, Sheldon FC, Prince SE, Calhoun VD, Doraiswamy PM. Default mode network connectivity in stable versus progressive mild cognitive impairment. Neurology. 2011;76:511–7.
39. Eichenbaum H. The hippocampus and declarative memory: cognitive mechanisms and neural codes. Behav Brain Res. 2001;127:199–207.
40. McKhann G, Drachman D, Folstein M, Katzman R, Price D, Stadlan EM. Clinical diagnosis of Alzheimer's disease: report of the NINCDS-ADRDA work group under the auspices of department of health and human services task force on Alzheimer's disease. Neurology. 1984;34:939–44.
41. Braak H, Braak E. Neuropathological stageing of Alzheimer-related changes. Acta Neuropathol. 1991;82:239–59.
42. Koch W, Teipel S, Mueller S, Buerger K, Bokde AL, Hampel H, et al. Effects of aging on default mode network activity in resting state fMRI: does the method of analysis matter? Neuroimage. 2010;51:280–7.
43. Johnson SC, Saykin AJ, Baxter LC, Flashman LA, Santulli RB, McAllister TW, et al. The relationship between fMRI activation and cerebral atrophy: comparison of normal aging and Alzheimer disease. Neuroimage. 2000;11:179–87.
44. Prvulovic D, Hubl D, Sack AT, Melillo L, Maurer K, Frolich L, et al. Functional imaging of visuospatial processing in Alzheimer's disease. Neuroimage. 2002;17:1403–14.
45. He Y, Wang L, Zang Y, Tian L, Zhang X, Li K, et al. Regional coherence changes in the early stages of Alzheimer's disease: a combined structural and resting-state functional MRI study. Neuroimage. 2007;35:488–500.
46. Cabeza R, Daselaar SM, Dolcos F, Prince SE, Budde M, Nyberg L. Task-independent and task-specific age effects on brain activity during working memory, visual attention and episodic retrieval. Cereb Cortex. 2004;14:364–75.
47. Daselaar SM, Fleck MS, Dobbins IG, Madden DJ, Cabeza R. Effects of healthy aging on hippocampal and rhinal memory functions: an event-related fMRI study. Cereb Cortex. 2006;16:1771–82.
48. Sharp DJ, Scott SK, Mehta MA, Wise RJ. The neural correlates of declining performance with age: evidence for age-related changes in cognitive control. Cereb Cortex. 2006;16:1739–49.
49. Otsuka Y, Osaka N, Morishita M, Kondo H, Osaka M. Decreased activation of anterior cingulate cortex in the working memory of the elderly. NeuroReport. 2006;17:1479–82.
50. Lustig C, Snyder AZ, Bhakta M, O'Brien KC, McAvoy M, Raichle ME, et al. Functional deactivations: change with age and dementia of the Alzheimer type. Proc Natl Acad Sci USA. 2003;100:14504–9.
51. Damoiseaux JS, Beckmann CF, Arigita EJ, Barkhof F, Scheltens P, Stam CJ, et al. Reduced resting-state brain activity in the "Default network" In normal aging. Cereb Cortex. 2008;18: 1856–64.
52. Andrews-Hanna JR, Reidler JS, Sepulcre J, Poulin R, Buckner RL. Functional–anatomic fractionation of the brain's default network. Neuron. 2010;65:550–62.
53. Minoshima S, Giordani B, Berent S, Frey KA, Foster NL, Kuhl DE. Metabolic reduction in the posterior cingulate cortex in very early Alzheimer's disease. Ann Neurol. 1997;42:85–94.
54. Marek T, Fafrowicz M, Golonka K, Mojsa-Kaja J, Oginska H, Tucholska K, et al. Diurnal patterns of activity of the orienting and executive attention neuronal networks in subjects performing a stroop-like task: a functional magnetic resonance imaging study. Chronobiol Int. 2010;27:945–58.
55. Shuter B, Yeh IB, Graham S, Au C, Wang SC. Reproducibility of brain tissue volumes in longitudinal studies: effects of changes in signal-to-noise ratio and scanner software. Neuroimage. 2008;41:371–9.
56. Ewers M, Teipel SJ, Dietrich O, Schonberg SO, Jessen F, Heun R, et al. Multicenter assessment of reliability of cranial MRI. Neurobiol Aging. 2006;27:1051–9.
57. Goto M, Abe O, Kabasawa H, Takao H, Miyati T, Hayashi N, et al. Effects of image distortion correction on voxel-based morphometry. Magn Reson Med Sci. 2012;11:27–34.
58. Goto M, Abe O, Miyati T, Kabasawa H, Takao H, Hayashi N, et al. Influence of signal intensity non-uniformity on brain volumetry using an atlas-based method. Korean J Radiol. 2012;13:391–402.

OPEN ACCESS Freely available online

PLOS | ONE

Comparison of Attenuation of Striated Muscle between Postmortem and Antemortem Computed Tomography: Results of a Longitudinal Study

Hidemi Okuma[1]*, Wataru Gonoi[1], Masanori Ishida[2], Go Shirota[1], Yukako Shintani[3], Hiroyuki Abe[3], Masashi Fukayama[3], Kuni Ohtomo[1]

1 Department of Radiology, Graduate School of Medicine, The University of Tokyo, Bunkyo-ku, Tokyo, Japan, **2** Department of Radiology, Mutual Aid Association for Tokyo Metropolitan Teachers and Officials, Sanraku Hospital, Chiyoda-ku, Tokyo, Japan, **3** Department of Pathology, Graduate School of Medicine, The University of Tokyo, Bunkyo-ku, Tokyo, Japan

Abstract

Objective: We evaluated the postmortem changes of striated muscle by comparing computed tomography (CT) images obtained postmortem and antemortem in the same patients.

Materials and Methods: We studied 33 consecutive patients who underwent antemortem CT, postmortem CT, and pathological autopsy in our tertiary care hospital between April 2009 and December 2010. Postmortem CT was performed within 20 h after death and was followed by pathological autopsy. Pathological autopsy confirmed the absence of muscular diseases such as amyotrophic lateral sclerosis, muscular dystrophy, myositis, and myasthenia, in all of the patients. The CT attenuation values of four cardiac muscle sites (anterior wall of the left ventricle, left ventricular free wall, posterior wall of the left ventricle, and the ventricular septum) and two skeletal muscle sites (the pectoralis major muscle and the erector spinae muscle) were compared between antemortem and postmortem CT using paired *t* test.

Results: Striated muscle had significantly greater attenuation on postmortem CT than on antemortem CT ($P<0.001$) in all six tissue sites. No significant association was found between postmortem change in the CT attenuation of striated muscle and gender, age, or elapsed time since death.

Conclusion: This is the first longitudinal study to show hyperattenuation of striated muscle on postmortem CT images compared with antemortem CT images in the same patients.

Citation: Okuma H, Gonoi W, Ishida M, Shirota G, Shintani Y, et al. (2014) Comparison of Attenuation of Striated Muscle between Postmortem and Antemortem Computed Tomography: Results of a Longitudinal Study. PLoS ONE 9(11): e111457. doi:10.1371/journal.pone.0111457

Editor: Hitoshi Okazawa, Tokyo Medical and Dental University, Japan

Received July 28, 2014; **Accepted** September 28, 2014; **Published** November 3, 2014

Data Availability: The authors confirm that all data underlying the findings are fully available without restriction. All relevant data are within the paper.

Funding: This work was supported by a grant from the Japanese Ministry of Health, Labor and Welfare, for research into "Usefulness of Postmortem Images as an Ancillary Method for Autopsy in Evaluation of Death Associated with Medical Practice (2008–2009)". The funders had no role in study design, data collection and analysis, decision to publish, or preparation of the manuscript.

Competing Interests: The authors have declared that no competing interests exist.

* Email: hokuma-tky@umin.ac.jp

Introduction

High-resolution imaging modalities such as computed tomography (CT) and magnetic resonance imaging are increasingly being used as adjuncts to traditional forensic methods in postmortem studies [1–5]. However, clinical radiologists may experience difficulty interpreting postmortem images because of specific and nonspecific postmortem signs [6]. As guidelines for the diagnosis of postmortem images are now being established worldwide, it is important to understand the normal changes on postmortem CT. The postmortem CT features of several organs have already been described [7–11]. To our knowledge, however, there are no reports describing the postmortem changes in CT attenuation of striated muscle. Therefore, we conducted a quantitative study in which we compared the attenuation of striated muscle between postmortem and antemortem CT in patients who died in hospital from nontraumatic causes. The results revealed significant difference in the attenuation of striated muscle between postmortem and antemortem CT.

Materials and Methods

Study design and donors

The Research Ethics Committee of the University of Tokyo Hospital approved this study, which was conducted in accordance with the principles of the Declaration of Helsinki. Written informed consent was obtained from the donor's next of kin to use the clinical, pathological, and radiographic data in this study. A total of 73 patients who died from nontraumatic causes in our academic tertiary care hospital and who underwent unenhanced chest antemortem CT, postmortem CT, and pathological autopsy between April 2009 and December 2010 were retrospectively

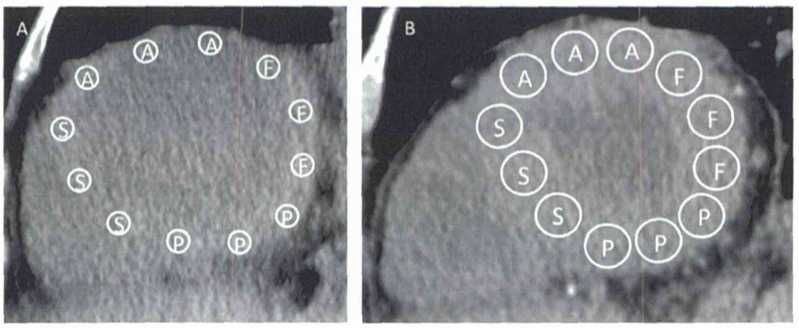

Figure 1. Antemortem and postmortem CT images of the heart in a representative patient. A: Multiplanar reconstruction image obtained by antemortem CT. B: Multiplanar reconstruction image obtained by postmortem CT. Both images were obtained in same plane. A, anterior wall of the left ventricle; F, left ventricular free wall; P, posterior wall of the left ventricle; S, ventricular septum.
doi:10.1371/journal.pone.0111457.g001

enrolled in this study. Potential donors were excluded for any of the following reasons: (a) age <20 years; (b) treatment with cardiopulmonary resuscitation; (c) diagnosis of congenital heart disease, chronic heart failure, cardiomyopathy, cardiac hypertrophy, or heart amyloidosis; prior cardiovascular surgery; or diagnosis of muscular disorders, such as amyotrophic lateral sclerosis, muscular dystrophy, myositis, or myasthenia. Criterion (c) was confirmed by pathological autopsy. After applying these exclusion criteria, 33 adult human cadavers (22 males, 11 females) were included in this study. The mean age at death was 66 years (range, 21–92 years; median, 72 years). All cadavers were placed in the supine position at room temperature from the time of death until postmortem CT. Antemortem CT was performed at a median of 17 days before death (range, 1–184 days). Postmortem CT was performed at a median of 464 min after death (range, 94–1175 min), followed by pathological autopsy.

Antemortem CT imaging

Antemortem CT scans were performed for reasons of clinical necessity such as for diagnosis or to ascertain the condition of hospitalized patients. All scans included at least the chest; patients were not excluded from the study if other regions of the body were scanned.

All antemortem CT studies were performed on 64-detector-row helical CT scanners (Aquilion 64, Toshiba Medical Systems Corporation, Ohtawara, Japan; Discovery CT750 HD and LightSpeed VCT, GE Healthcare, Buckinghamshire, UK) in the craniocaudal direction with the patient in the supine position with both arms raised. The scan parameters were as follows: slice thickness, 5 mm; slice interval, 5 mm; rotation time, 0.5 s; and tube voltage, 120 kVp. Automatic tube current modulation was performed by Volume EC (Toshiba) and AutomA (GE). Images were reconstructed at 0.5 mm intervals with a 350 mm field of view and a 512×512 image matrix.

Postmortem CT imaging

Postmortem CT scans of the whole body were performed to examine the cause of death.

All postmortem CT studies were performed without contrast medium on a 4-detector-row CT scanner (Robusto, Hitachi Medical Corporation, Tokyo, Japan) in helical mode, in the craniocaudal direction. For all scans, the cadaver was laid in the supine position with arms placed on either side of the body. The scan parameters were as follows: slice thickness, 2.5 mm; slice interval, 1.25 mm; rotation time, 0.5 s; tube voltage, 120 kVp; and tube current, 250 mA. Images were reconstructed at 1.25 mm intervals with a 350 mm field of view and a 512×512 image matrix.

Image interpretation

All images were interpreted by a radiologist who was not provided with clinical information. The postmortem and most recent antemortem unenhanced chest CT images were compared. CT images were reviewed on a three-dimensional workstation (ZioTerm2009, Ziosoft, Inc., Tokyo, Japan) to obtain multiplanar reconstruction images perpendicular to the line transecting the

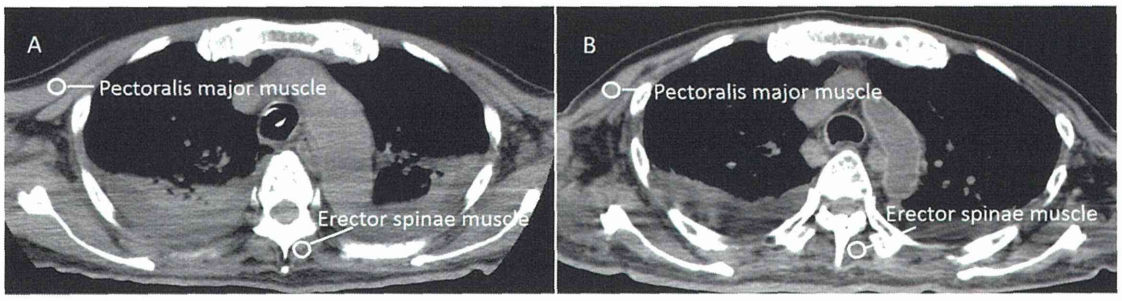

Figure 2. Antemortem and postmortem CT images of the pectoralis major muscle and the erector spinae muscle in a representative patient. A: Antemortem CT. B: Postmortem CT. Both images were obtained at the level of the aortic arch. PMM, pectoralis major muscle; ESM, erector spinae muscle.
doi:10.1371/journal.pone.0111457.g002

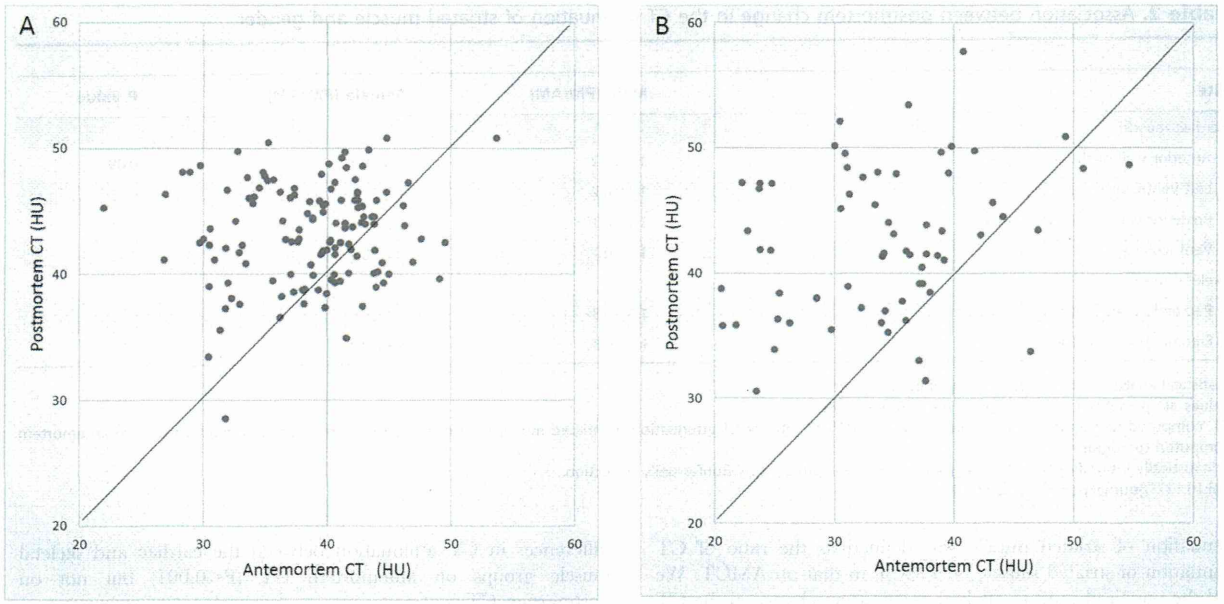

Figure 3. Scatter plot of the CT attenuation values of cardiac and skeletal muscle on antemortem and postmortem CT. A: Cardiac muscle. B: Skeletal muscle.
doi:10.1371/journal.pone.0111457.g003

apex and the center of the mitral valve. A slice at approximately one third of the distance from the apex, corresponding to a pathological section of the heart, was chosen for the analysis. Using the multiplanar reconstruction images, we measured CT attenuation (in Hounsfield units; HU) at three points in each of the following four cardiac muscle sites: anterior wall of the left ventricle, left ventricular free wall, posterior wall of the left ventricle, and the ventricular septum (Fig. 1A,B). The mean values of the three points at each site were calculated. The CT attenuation (in HU) was also determined for the pectoralis major muscle and the erector spinae muscle at the level of the aortic arch (Fig. 2A,B). CT attenuation was measured by setting a circular region of interest (ROI) to the center of each muscle. ROI size was as large as possible without being affected by partial volume phenomena, and the average CT attenuation within the ROI was used for analysis.

Statistical analyses

We compared the CT attenuation of six sites of striated muscle (i.e., four cardiac muscle sites: anterior wall of the left ventricle, left ventricular free wall, posterior wall of the left ventricle, ventricular septum; and two skeletal muscle sites: pectoralis major muscle and erector spinae muscle) between antemortem CT and postmortem CT using paired t tests. Significant differences among the four cardiac muscle sites were determined using Friedman's test. Significant differences between the two skeletal muscle sites were determined using the paired t tests. Significant differences between the group of cardiac muscles and that of skeletal muscles were analyzed by unpaired t tests. Postmortem change in the CT

Table 1. Comparison of striated muscle attenuation in four cardiac muscle sites, the pectoralis major muscle, and the erector spinae muscle, between antemortem CT and postmortem CT.

Site	Antemortem CT attenuation (HU)	Postmortem CT attenuation (HU)	*P* value*
Cardiac muscle			
Anterior wall of the left ventricle	36.8±6.2	42.5±4.6	<0.001
Left ventricular free wall	38.1±6.2	44.1±3.7	<0.001
Posterior wall of the left ventricle	40.0±3.8	43.8±3.7	<0.001
Ventricular septum	39.6±3.4	42.5±3.2	<0.001
Skeletal muscle			
Pectoralis major muscle	33.7±6.8	43.3±5.9	<0.001
Erector spinae muscle	34.1±8.0	41.7±5.6	<0.001

Values are presented as the mean ± standard deviation.
*Paired t tests.
CT, computed tomography; HU, Hounsfield units.
doi:10.1371/journal.pone.0111457.t001

Table 2. Association between postmortem change in the CT attenuation of striated muscle and gender.

Site	Male (PM/AM)	Female (PM/AM)	P value
Cardiac muscle			
Anterior wall of the left ventricle	1.1±0.2	1.3±0.3	0.09
Left ventricular free wall	1.1±0.2	1.3±0.2	0.03#
Posterior wall of the left ventricle	1.1±0.1	1.2±0.2	0.04#
Ventricular septum	1.1±0.1	1.1±0.1	0.10
Skeletal muscle			
Pectoralis major muscle	1.3±0.3	1.1±0.3	0.08
Erector spinae muscle	1.4±0.3	1.3±0.3	0.29

Statistical analyses were performed by unpaired t-test.
Values are presented as the mean ± standard deviation.
CT, computed tomography; HU, Hounsfield units; PM/AM, ratio of CT attenuation of striated muscle on postmortem computed tomography to that on antemortem computed tomography.
#Statistically insignificant when family-wise error was corrected by Bonferroni's correction.
doi:10.1371/journal.pone.0111457.t002

attenuation of striated muscle was defined as the ratio of CT attenuation of striated muscle on PMCT to that on AMCT. We used the unpaired t-test to analyze postmortem change in the CT attenuation of striated muscle with gender, and linear least squares regression for that with age and elapsed time since death. The level of statistical significance was set at 0.05. Family-wise error was corrected by Bonferroni's correction for each section. All statistical analyses were performed using R version 3.0 (The R Foundation for Statistical Computing, Vienna, Austria; http://www.r-project.org/).

Results

The CT attenuation values (in HU) of the four cardiac muscle sites and the two skeletal muscle sites on antemortem and postmortem CT are shown in a scatter plot (Fig. 3A,B). These results are also summarized in Table 1. Both cardiac and skeletal muscle showed significantly greater attenuation on postmortem CT than on antemortem CT. The Friedman test showed that there were no significant differences in CT attenuation among the four sites of cardiac muscle either on antemortem or on postmortem CT. There were also no significant differences in CT attenuation between the two sites of skeletal muscle either on antemortem or on postmortem CT. There were significant differences in CT attenuation between the cardiac and skeletal muscle groups on antemortem CT ($P<0.001$) but not on postmortem CT.

Table 2 summarizes the association of postmortem change in the CT attenuation of striated muscle with gender. Gender showed no statistically significant association with postmortem change in the CT attenuation of striated muscle, at any of the tested sites.

Table 3 shows the results of correlation analysis for postmortem change in the CT attenuation of striated muscle with each of age and elapsed time since death. No statistically significant correlation was found at any site.

Discussion

Although several studies have evaluated the postmortem changes of the cardiovascular system [12–17], few studies have examined the changes in CT attenuation. Shiotani et al. [12] reported that the attenuation of the aortic wall was greater on postmortem CT than on antemortem CT. They also reported that compression of aortic wall components, including collagen fibers, elastic fibers, and smooth muscle, may contribute to the hyperattenuation on postmortem CT. Okuma et al. [15] reported that the heart wall is thicker on postmortem CT than on

Table 3. Correlation of association between postmortem change in the CT attenuation of striated muscle with age and with elapsed time since death.

Site	Age	Elapsed time since death
Cardiac muscle		
Anterior wall of the left ventricle	0.79	0.12
Left ventricular free wall	0.98	0.34
Posterior wall of the left ventricle	0.30	0.05
Ventricular septum	0.38	0.32
Skeletal muscle		
Pectoralis major muscle	0.09	0.45
Erector spinae muscle	0.51	0.34

Statistical analyses were performed by linear least squares regression.
CT, computed tomography.
doi:10.1371/journal.pone.0111457.t003

antemortem CT, which suggests that postmortem contraction of cardiac muscle may cause increase the attenuation of cardiac muscle on postmortem images, as observed in our study.

In the present study, the CT attenuation of the pectoralis major muscle and the erector spinae muscle was significantly greater on postmortem CT than on antemortem CT in the same patients. Lewy et al. [18] reported that postmortem CT did not depict findings specific for rigor mortis, and that rigor did not affect CT attenuation, or the size and shape of skeletal muscles. However, it is well known in the fields of forensic medicine and pathology that rigor mortis causes contraction of striated muscle [19]. Because CT attenuation is affected by the density of muscle [20], the greater attenuation on postmortem CT than on antemortem CT is consistent with the contraction of striated muscle in rigor mortis.

There were no significant intra-group (among the four cardiac muscle sites or between the two skeletal muscle sites) differences in CT attenuation either on antemortem or postmortem CT. Even though they are named differently, the properties of cardiac muscle at different sites in the heart can be quite similar. Regarding the two sites of skeletal muscle, the pectoralis major and erector spinae muscles may also show similar CT attenuation values. Muscles are known to exhibit broad regional differences in muscle fiber density [21,22] and in CT attenuation [23,24]. We would have observed a wider variety of CT attenuation values in the group of skeletal muscle if more muscle regions had been added to the analysis.

Antemortem CT attenuation was significantly different between the cardiac and skeletal muscle groups. Because of the marked differences in cardiac and skeletal muscle in terms of their physiological properties as well as their pathological responses, the difference in CT attenuation between these two categories of muscle could reflect these differences in properties. The broad regional differences in muscle fiber density [21,22] and CT attenuation [23,24] mentioned earlier mean that the significant differences in antemortem CT attenuation among muscles in different regions detected in this study are to be expected. Although Bulcke et al. [23] and Termote et al. [24] reported similar findings—that the sternocleidomastoideus and iliopsoas are characterized by high attenuation and the gracilis and triceps surae are characterized by low attenuation—there were large differences in the measured CT values for the same muscles. Therefore, we cannot compare the absolute values determined in this study with those of previous studies.

Somewhat unexpectedly, we found no significant differences in postmortem CT attenuation between the cardiac and skeletal muscle groups. One possible explanation is that rigor mortis resulted in marked contraction of the striated muscles, abolishing any possible differences between individual striated muscles on postmortem CT.

If rigor mortis is the principal cause of the hyperattenuation of striated muscle on PMCT, then postmortem change in the CT attenuation of striated muscle should be associated with elapsed time since death, because the presence and degree of rigor mortis generally changes in the period between 1–2 hours and between 24–36 hours after death [25]. In the present study, all PMCT scanning was performed between 1.5 and 20 hours post mortem, which coincides with the timing of rigor mortis. However, our results revealed few associations between postmortem change in the CT attenuation of striated muscle and elapsed time since death. One possibility for this finding is that the total number of patients analyzed in the study was too small to show a positive association.

We also investigated possible confounding factors of postmortem change such as gender and age. The associations between these factors and postmortem change in the CT attenuation of striated muscle were not statistically significant, which indicates that hyperattenuation of striated muscle is a general postmortem finding regardless of gender or age.

Interscanner variability of CT attenuation values (i.e., HU) is an issue that needs to be considered [26,27], although almost all CT scanners show some intrascanner variability in CT attenuation values [28]. Recent technological innovations, however, may overcome these problems because some studies have shown negligible interscanner variability in terms of CT attenuation values [29]. Although CT attenuation values may not be directly compared between antemortem and postmortem CT because we used different scanners at each time, we fixed the tube voltage at 120 kVp, which should help to reduce the variability. Of course, the significant differences in CT attenuation values between antemortem and postmortem CT cannot be explained without considering postmortem changes if there is any interscanner or intrascanner variability.

Our study has some other limitations. Motion artifacts from the heart may affect antemortem CT but do not affect postmortem CT. It is also possible that underlying diseases, cadaver preservation, atmospheric conditions (e.g. temperature or humidity), or other factors might contribute to the differences observed postmortem [30,31]. However, some of these factors are unlikely to affect our conclusions because we excluded patients with cardiovascular or muscular diseases from the study, which was confirmed by the pathological autopsy, and all of the cadavers were preserved in accordance with the regulations used at our hospital.

Conclusions

This is the first longitudinal study to show that striated muscle exhibits significantly greater attenuation on postmortem CT than on antemortem CT in patients who died in hospital from nontraumatic causes.

Author Contributions

Conceived and designed the experiments: HO WG MI GS. Performed the experiments: HO WG MI GS. Analyzed the data: HO WG. Contributed reagents/materials/analysis tools: YS HA MF. Wrote the paper: HO WG KO.

References

1. Thali MJ, Yen K, Schweitzer W, Vock P, Boesch C, et al. (2003) Virtopsy, a new imaging horizon in forensic pathology: virtual autopsy by postmortem multislice computed tomography (MSCT) and magnetic resonance imaging (MRI) – a feasibility study. J Forensic Sci 48: 386–403.
2. O'Donnell C, Woodford N (2008) Post-mortem radiology - a new sub-speciality? Clin Radiol 63: 1189–1194.
3. Cha JG, Kim DH, Paik SH, Park JS, Park SJ, et al. (2010) Utility of postmortem autopsy via while-body imaging: initial observations comparing MDCT and 3.0 T MRI findings with autopsy findings. Korean J Radiol 11: 395–406.
4. Roberts IS, Benamore RE, Benbow EW, Lee SH, Harris JN, et al. (2012) Postmortem imaging as an alternative to autopsy in the diagnosis of adult deaths: a validation study. Lancet 379: 136–142.
5. Flach PM, Thali MJ, Germerott T (2014) Times have changed! Forensic radiology - a new challenge for radiology and forensic pathology. Am J Roentgenol 202: W325–W334.
6. Christe A, Flach P, Ross S, Spendlove D, Bolliger S, et al. (2010) Clinical radiology and postmortem imaging (Virtopsy) are not the same: Specific and unspecific postmortem signs. Leg Med (Tokyo) 12: 215–222.

7. Shiotani S, Kohno M, Ohashi N, Yamazaki K, Nakayama H, et al. (2004) Non-traumatic postmortem computed tomographic (postmortem CT) findings of the lung. Forensic Sci Int 139: 39–48.
8. Ishida M, Gonoi W, Hagiwara K, Takazawa Y, Akahane M, et al. (2011) Intravascular gas distribution in the upper abdomen of non-traumatic in-hospital death cases on postmortem computed tomography. Leg Med (Tokyo) 13: 174–179.
9. Ishida M, Gonoi W, Hagiwara K, Takazawa Y, Akahane M, et al. (2011) Hypostasis in the heart and great vessels of non-traumatic in-hospital death cases on postmortem computed tomography: relationship to antemortem blood tests. Leg Med (Tokyo) 13: 280–285.
10. Ishida M, Gonoi W, Hagiwara K, Takazawa Y, Akahane M, et al. (2011) Postmortem changes of the thyroid on computed tomography. Leg Med (Tokyo) 13: 318–322.
11. Ishida M, Gonoi W, Hagiwara K, Okuma H, Shintani Y, et al. (2014) Fluid in the airway of nontraumatic death on postmortem computed tomography: relationship with pleural effusion and postmortem elapsed time. Am J Forensic Med Pathol 35: 113–117.
12. Shiotani S, Kohno M, Ohashi N, Yamazaki H, Nakayama H, et al. (2002) Hyperattenuating aortic wall on postmortem computed tomography (postmortem CT). Radiat Med 20: 201–206.
13. Shiotani S, Kohno M, Ohashi N, Yamazaki K, Nakayama H, et al. (2003) Dilation of the heart on postmortem computed tomography (postmortem CT): comparison with live CT. Radiat Med 21: 29–35.
14. Hyodoh H, Sato T, Onodera M, Washio H, Hasegawa T (2012) Vascular measurement changes observed using postmortem computed tomography. Jpn J Radiol 30: 840–845.
15. Okuma H, Gonoi W, Ishida M, Shintani Y, Takazawa Y, et al. (2013) Heart wall is thicker on postmortem computed tomography than on ante mortem computed tomography: the first longitudinal study. PLoS One 8: e76026.
16. Okuma H, Gonoi W, Ishida M, Shintani Y, Takazawa Y, et al. (2013) Greater thickness of the aortic wall on postmortem computed tomography compared with antemortem computed tomography: the first longitudinal study. Int J Legal Med In press; doi: 10.1007/s00414-013-0955-z.
17. Takahashi N, Higuchi T, Hirose Y, Yamanouchi H, Takatsuka H (2013) Changes in aortic shape and diameters after death: comparison of early postmortem computed tomography with antemortem computed tomography. Forensic Sci Int 225: 27–31.
18. Lewy AD, Harcke HT, Mallak CT (2010) Postmortem imaging: MDCT features of postmortem change and decomposition. Am J Forensic Med Pathol 31: 12–17
19. Smith RD (1950) Studies on rigor mortis, Part 2, Qualitative observations on the post mortem shortening of muscles. Anat Rec 108: 207–216.
20. Mull RT (1984) Mass estimates by computed tomography: physical density from CT numbers. AJR Am J Roentgenol 143: 1101–1104.
21. Hadar H, Gadoth N, Heifetz M (1983) Fatty replacement of lower paraspinal muscles: normal and neuromuscular disorders. AJR Am J Roentgenol 141: 895–898.
22. Hawley RJ Jr, Schellinger D, O'Doherty DS (1984) Computed tomographic patterns of muscles in neuromuscular diseases. Arch Neurol 41: 383–387.
23. Bulcke JA, Termote JL, Palmers Y, Crolla D (1979) Computed tomography of the human skeletal muscular system. Neuroradiology 17: 127–136.
24. Termote JL, Baert A, Crolla D, Palmers Y, Bulcke JA (1980) Computed tomography of the normal and pathologic muscular system. Radiology 137: 139–144.
25. Tsokos M (2005) Postmortem changes. In: Payne-James J, Byard RW, Corey TS and Henderson C, editors.Encyclopedia of forensic and legal medicine.Oxford: Elsevier Academic Press. pp.456–476.
26. Levi C, Gray JE, McCullough EC, Hattery RR (1982) The unreliability of CT numbers as absolute values. AJR Am J Roentgenol 139: 443–447.
27. Groell R, Rienmueller R, Schaffler GJ, Portugaller HR, Graif E, et al. (2000) CT number variations due to different image acquisition and reconstruction parameters: a thorax phantom study. Comput Med Imaging Graph 24: 53–58.
28. Birnbaum BA, Hindman N, Lee J, Babb JS (2007) Multi-detector row CT attenuation measurements: assessment of intra- and interscanner variability with an anthropomorphic body CT phantom. Radiology 242: 109–119.
29. Nishihara S, Koike M, Ueda K, Sanada T, Ebitani K, et al. (2002) Intra- and inter-equipment variations in the mean CT numbers of a vertebral body for X-ray CT equipment. Med Imag Inform Sci 20: 40–43 (in Japanese).
30. Jackowski C, Sonnenschein M, Thali MJ, Aghayev E, Yen K, et al. (2007) Intrahepatic gas at postmortem computed tomography: forensic experience as a potential guide for in vivo trauma imaging. J Trauma 62: 979–988.
31. Singh MK, O'Donnell C, Woodford NW (2009) Progressive gas formation in a deceased person during mortuary storage demonstrated on computed tomography. Forensic Sci Med Pathol 5: 236–242.

フォーラム

治験開始前のサンプル検査データ提出における適切な同意取得方法の確立

山田奈央子* 玉見康江* 渡部歌織*
戸田智恵子* 青木敦* 河原崎秀一*
上田哲也* 山崎力* 荒川義弘*

Establishment of Standardized Procedures to Obtain Informed Consent for Submission of Sample Examination Data before Starting Trials

Naoko YAMADA, Yasue TAMAMI, Kaori WATANABE, Chieko TODA, Atsushi AOKI, Shuichi KAWARAZAKI, Tetsuya UEDA, Tsutomu YAMAZAKI and Yoshihiro ARAKAWA

Clinical Research Support Center, The University of Tokyo Hospital, Japan

An increasing number of clinical trials recently require the submission of examination data as sample to check the feasibility of the study before the trials are started. However, procedures to obtain informed consent have not been standardized. Therefore, we investigated various procedures by reviewing past cases and guidelines on research ethics and personal information protection. Based on this review, we developed the procedures for four types of study classified according to the prospective nature and degree of invasiveness of the examination. In type A, when the sample data is prospective and requires implementation of invasive examination not conducted as part of routine medical care, written informed consent is mandatory and each examination must be approved by the institutional review board (IRB). In type B, when the sample data is prospective and requires implementation of less invasive or non-invasive examination not conducted as part of routine medical care, use of pre-approved template of written informed consent that includes explanations of foreseeable risks and inconveniences accompanying the examination is required. In type C, when the sample data is prospective and uses results of examination conducted as part of routine medical care, informed consent can be obtained either orally or in writing at the discretion of the investigator. In type D, when the sample data uses preexisting medical data, efforts have to be made to obtain oral informed consent as far as possible. However, if informed consent is not possible, individual informed consent can be omitted but general notice should be given to patients regarding use of their medical records for purposes including answering inquires on medical services from other medical institutions. This classification system, which includes flowcharts and templates for informed consent, has been approved by the IRB at the University of Tokyo Hospital and will facilitate proper handling of sample data.

Key words: clinical trials, sample data, informed consent, ethical guidelines, privacy protection

Jpn J Clin Pharmacol Ther. 2015; 46(1): 21-27

1．背景・目的

近年，施設調査の一環として，検査を行う医療従事者の技能評価や適正なデータ解析の可否判定など，試験データの質を保証するために，試験開始前にサンプルとして検査データ（以下，サンプル検査データ）の提出が規定されている試験が増加してきている．提出するサンプル検査データはさまざまであり，すでに実施された検査で得られたデータで対応可能なものや，日常診療では行わない試験特有の手順どおりに実施することが求められることもある．

このサンプル検査データの提出は，研究の前段階として，検査の品質の確認のために行うもので，研究そのものではない．しかしながら，日常診療の外で研究に紐づいて実施するものであり，データの利用や侵襲的検査の実施については，協力者の同意や倫理的検討を要する行為であると考えられる．

そこで，本研究課題では既存の倫理指針等を参考に，既存資料であるか否かや侵襲的であるか否かにより分類し，そのうち，低侵襲の検査の場合や既存資料を利用する場合については，円滑かつ適切に進めるための同意取得方法について検討し，これらすべての手順について Institutional

* 東京大学医学部附属病院臨床研究支援センター
著者連絡先：山田奈央子 東京大学医学部附属病院臨床研究支援センター 〒113-8655 東京都文京区本郷 7-3-1
E-mail：ymd-na@umin.ac.jp
投稿受付 2014 年 9 月 2 日，第 2 稿受付 2014 年 10 月 27 日，掲載決定 2014 年 10 月 31 日
ISSN 0388-1601

Table 東大病院におけるヒトを対象とした検査のサンプルデータ提出状況（2010年4月～2013年5月）
提出するサンプル検査データの想定されるパターンは4種（前向き or 後向き，患者 or 健常人，この試験のために実施 or 日常診療でも必要，低侵襲 or 高侵襲）であることが推察された．

受託診療科	検査項目	データ取得	検査対象者の規定	侵襲性	同意取得方法
眼科・視覚矯正科	・眼底カメラ撮影 ・眼底三次元画像解析（OCT）	前向き	あり （対象疾患の患者* および健常対照）	低	文書IC
眼科・視覚矯正科					
眼科・視覚矯正科					
眼科・視覚矯正科	・眼底カメラ撮影 ・眼底三次元画像解析（OCT）	前向き	あり （対象疾患の患者*）	低	口頭IC
	眼底カメラ撮影（蛍光眼底法）	前向き	あり （対象疾患の患者*）	高	口頭IC
循環器内科	右心カテーテル	後向き（既存データ）	なし	—	文書IC
	心エコー	前向き	なし	低	口頭IC
神経内科	嚥下造影	後向き（既存データ）	なし	—	文書IC
腎臓・内分泌内科	骨塩量（DXA法）	後向き（既存データ）	なし	—	IC なし
アレルギー・リウマチ内科	血圧	前向き	なし	低	口頭IC
消化器内科	・単純MRI ・心エコー	前向き	なし	低	口頭IC
糖尿病・代謝内科	24時間自由行動下血圧	前向き	なし	低	口頭IC
眼科・視覚矯正科	・眼底カメラ撮影 ・眼底三次元画像解析（OCT）	前向き	あり （対象疾患の患者* および健常対照）	低	文書IC
眼科・視覚矯正科	眼底カメラ撮影（蛍光眼底法）	前向き	あり （対象疾患の患者* および健常対照）	高	文書IC

＊：日常診療においてを検査する必要があった患者さんにご協力いただいた．

Review Board（IRB）にてその妥当性を諮った．そこで，このたび確立したサンプル検査データを提出する際の適切な同意取得方法について報告する．

2．方　法

2.1. 過去の事例により想定されるパターンの検討

協力者の同意に影響する要因として，検査内容（とくに侵襲性の程度），既存データであるか，前向きに取得するものであるか，日常診療で得られるデータであるか等が推察される．そこで，これまでに東京大学医学部附属病院（以下，東大病院）において対応した事例について調査し，提出するサンプル検査データについて想定されるパターンを検討する．

2.2. 関連法規の参照

倫理指針や個人情報保護に関連したガイドラインを参考にし，サンプル検査データの取扱いや同意取得方法について検討する．

2.3. 対応方法の確立

2.1.，2.2. で検討した結果を踏まえ，適切な対応方法を策定し，IRBに承認を得る．

3．結　果

3.1. 過去の事例により想定されるパターンの検討

2010年度～2013年5月の東大病院における治験および製造販売後臨床試験の新規受託試験数は2010年度33試験，2011年度39試験，2012年度43試験，2013年度（5月まで）は14試験であった．この間に東大病院においてサンプル検査データを提出した事例について調査した（**Table**）．

ヒトを対象とした検査のサンプルデータを提出した項目数はのべ16項目であり，眼科的検査など画像検査が多かった．既存データ提出での対応項目数は3項目，前向きに取得した項目数は13項目であった．後者のほうが項目数が多かった要因としては，各試験において規定された検査手順は日常診療における手順と細かい点で異なることが多く，規定の手順どおりに検査を実施し，適切なデータを提出可能か否か判断するためには，前向きデータが必要となるためと考えられた．

対象データについては，規定がなく，健常人データの提